Phytochemistry 226 (2024) 114225

Contents lists available at ScienceDirect

Phytochemistry

journal homepage: www.elsevier.com/locate/phytochem

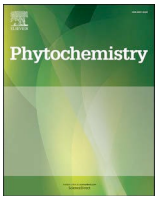

Identification of substituted variants of plastoquinone-9 as potent and specific photosynthetic inhibitors in cyanobacteria and plants

Scott Latimer **, Lauren R. Stutts , Gilles J. Basset *

Department of Horticultural Sciences, University of Florida, Gainesville, FL, 32611, USA

ARTICLE INFO

Keywords:
Herbicide
Algicide
Plastoquinone
Duroquinone
Benzoquinone
Cyanobacteria
Plastids

ABSTRACT

The unprenylated benzoquinones 2,3,5,6-tetramethyl-1,4-benzoquinone (duroquinone), 2-chloro-1,4-benzoquinone (CBQ), 2,6-dimethyl-1,4-benzoquinone (DMBQ), 2,6-dichloro-1,4-benzoquinone (DCBQ), and 2,6-dimethoxy-1,4-benzoquinone (DMOBQ) were tested as putative antimetabolites of plastoquinone-9, a vital electron and proton carrier of oxygenic phototrophs. Duroquinone and CBQ were the most effective at inhibiting the growth of the cyanobacterium *Synechocystis* sp. PCC 6803 either in photomixotrophic or photoautotrophic conditions. Duroquinone, a close structural analog of the photosynthetic inhibitor methyl-plastoquinone-9, was found to possess genuine bactericidal activity towards *Synechocystis* at a concentration as low as 10 μM, while at the same concentration CBQ acted only as a mild bacteriostat. In contrast, only duroquinone displayed marked cytotoxicity in axenically-grown Arabidopsis, resulting in damages to photosystem II and hindered net CO_2 assimilation. Metabolite profiling targeted to photosynthetic cofactors and pigments indicated that in Arabidopsis duroquinone does not directly inhibit plastoquinone-9 biosynthesis. Taken together, these data indicate that duroquinone offers prospects as an algicide and herbicide.

1. Introduction

Blooms of toxin-producing cyanobacteria are a widespread problem for freshwater and marine environments as well as for the sourcing of drinking water, and raising temperatures associated with climate change increasingly compound the issue (Huisman et al., 2018; Kosten et al., 2012; Paerl and Paul, 2012). While short-term curative treatments using copper or hydrogen peroxide can be used to quickly mitigate cyanobacterial blooms, these methods often lead to the release of cyanotoxins from the dying cells and exacerbate water pollution (Merel et al., 2013; Lürling et al., 2014). Prevention of cyanobacterial blooms (*e.g.* via nutrient reduction) is therefore the preferred control method (Lürling et al., 2014). Similarly, herbicide-resistant weeds represent a major challenge to agriculture, threatening crop production and global food security worldwide (Powles and Yu, 2010; Peterson et al., 2018). In particular, the emergence of cross resistance and multiple resistance to herbicides often results in labor intensive and costly management practices, such as tilling, selective weed removal, and use of cover crops (Sosnoskie and Culpepper, 2014; Gerhards et al., 2016). Understandably, potent and safe inhibitors of photosynthesis harboring new modes of action are in strong demand (Duke and Dayan, 2022).

Studies have shown that interfering with the functions of the electron and proton carrier plastoquinone-9, either via usage of competitive inhibitors or blockage of plastoquinone-9 biosynthesis, can result in complete inhibition of photosynthesis (Boler et al., 1972; Block et al., 2014; Kahlau et al., 2020). Plastoquinone-mediated electron transfer is also the target of a large group of herbicides, including DCMU (diuron), atrazine, metribuzin, phenisopham, and phenmedipham, that bind to the Q_B site of the D1 protein of photosystem II and block the electron flow originating from Q_A (Tischer and Strotmann, 1977; Oettmeier et al., 1984; Metz et al., 1986).

Our group has recently uncovered the existence in cyanobacteria and plastids of a selection pressure that prevents the enzyme demethylnaphthoquinol *C*-methyltransferase from cross-reacting with plastoquinone-9 (Stutts et al., 2023). Specifically, this study demonstrated that expression of a substrate promiscuous quinol *C*-methyltransferase in the cyanobacterium *Synechocystis* sp. PCC 6803 or in the plastids of *Arabidopsis thaliana* (L.) Heynh (Brassicaceae) resulted in the

Abbreviations: CBQ, 2-Chloro-1,4-benzoquinone; DMBQ, 2,6-Dimethyl-1,4-benzoquinone; DCBQ, 2,6-Dichloro-1,4-benzoquinone; DCMU, N′-(3,4-dichlorophenyl)-N,N-dimethylurea; DMOBQ, 2,6-Dimethoxy-1,4-benzoquinone; FW, Fresh weight; HPLC, High performance liquid chromatography; PSII, Photosystem II.

* Corresponding author. Plant Molecular & Cellular Biology Program University of Florida, 1109 Fifield Hall P.O. Box 110690, Gainesville, FL, 32611, USA.
** Corresponding author. Plant Molecular & Cellular Biology Program University of Florida, 1109 Fifield Hall P.O. Box 110690, Gainesville, FL, 32611, USA.
E-mail addresses: scottlatimer@ufl.edu (S. Latimer), laurenrstutts@ufl.edu (L.R. Stutts), gbasset@ufl.edu (G.J. Basset).

https://doi.org/10.1016/j.phytochem.2024.114225
Received 2 May 2024; Received in revised form 15 July 2024; Accepted 18 July 2024
Available online 19 July 2024

production of a new-to-nature and acutely cytotoxic methylated variant of plastoquinone-9 (Fig. 1; Stutts et al., 2023). Analyses of the corresponding *Synechocystis* transformants and Arabidopsis transgenics indicated that methyl-plastoquinone-9 was not only unable to function as an electron carrier *in vivo*, but also acted as an inhibitor of plastoquinone-9 (Stutts et al., 2023). The present work leverages the basic knowledge gained from our recent findings on the evolution of quinol *C*-methyltransferase in oxygenic phototrophs to search for synthetic benzoquinones as potential new algicides and herbicides.

2. Results and discussion

2.1. Unprenylated benzoquinones inhibit the growth of Synechocystis depending on the type of ring substitutions and growth conditions

As previous studies indicated that unprenylated quinones and phenolics were readily absorbed and metabolized when supplied to cyanobacterial and plant cultures (Widhalm et al., 2009; Block et al., 2014; Nowicka and Kruk, 2016), five unprenylated benzoquinones were selected for pilot growth assays with the cyanobacterium *Synechocystis* sp. PCC6803. These compounds include 2,3,5,6-tetramethyl-1,4-benzoquinone (duroquinone), 2-chloro-1,4-benzoquinone (CBQ), 2,6-dimethyl-1,4-benzoquinone (DMBQ), 2,6-dichloro-1,4-benzoquinone (DCBQ), and 2,6-dimethoxy-1,4-benzoquinone (DMOBQ). Of those, duroquinone is the most closely related to cytotoxic methyl-plastoquinone-9, the two molecules differing solely by the decoration of carbon 5: duroquinone is methylated at this position, while methyl-plastoquinone harbors a solanesyl (C45) chain (Fig. 1; Fig. 2A). That duroquinone's ring is fully substituted thus precludes a priori its prenylation *in vivo* (Fig. 2A). In contrast, the four other benzoquinones display two (DMBQ, DMOBQ, DCBQ) to three (CBQ) unsubstituted carbons, which are available, at least in theory, for prenylation *in vivo* (Fig. 2A). There exist precedents for such prenylation of exogenously fed aromatic and quinoid molecules in cyanobacteria as well as in plants (Widhalm et al., 2009; Block et al., 2014; Nowicka and Kruk, 2016).

With the exception of DMOBQ, whose low solubility prevented its testing beyond 10 μM in our experimental setup, all benzoquinones displayed various extent of growth inhibition activity when added to photomixotrophic cultures of *Synechocystis* (Fig. 2A). Cell growth was either fully or markedly inhibited at 25 μM, but not at 10 μM, for DMBQ and DCBQ, respectively (Fig. 2A). No growth was observed for cultures containing CBQ or duroquinone, either at 10 μM or 25 μM (Fig. 2A). Similar results were obtained when growth assays were conducted in photoautotrophic conditions, albeit doubling times of photoautrophic cultures were 6–7 times lower than that of their photomixotrophic counterparts, and some cell growth was observed at 25 μM DMBQ (Fig. 2B). Of all the tested benzoquinone variants, CBQ and duroquinone appear therefore to be the most effective at inhibiting the growth of *Synechocystis*.

2.2. Duroquinone and CBQ act as bactericide and bacteriostat on Synechocystis, respectively

To establish if the underlying cytotoxicity of CBQ and duroquinone resulted from bactericidal or bacteriostatic activity, photomixotrophic cultures in exponential phase (T48 h) were spiked with CBQ and duroquinone, each at a final concentration of 10 μM (Fig. 3A). CBQ addition resulted in a temporary decrease in growth rate of ~30% (T72 h) as compared to the mock treatment (Fig. 3A). Within ~24 h (T96 h) CBQ-containing cultures reached the same stationary OD as that of the control (Fig. 3A). In contrast, addition of duroquinone to *Synechocystis* cultures abruptly halted cell growth (Fig. 3A). Furthermore, within 24 h following duroquinone addition (T72 h), cells developed an increasingly paler green pigmentation as compared to their color at the beginning of the treatment, and by T144 h these cells were fully bleached (Fig. 3B). Control and CBQ-treated *Synechocystis* cells, on the other hand, maintained their characteristic dark green hue (Fig. 3B).

In parallel, cells were harvested from culture aliquots immediately prior to (T48 h) and 24 h after (T72 h) the addition of CBQ and duroquinone (Fig. 3A). Cell pellets were washed, and resuspended cells were then plated via serial dilutions on photomixotrophic medium (Fig. 3C). After 9 days of culture, inocula corresponding to CBQ-exposed *Synechocystis* cells displayed a slight decrease in colony density as compared to the mock-treated cells; this was most visible at the 10^{-2} and 10^{-3} dilutions (Fig. 3C). In stark contrast, almost no growth was observed for duroquinone-exposed *Synechocystis* cells and inocula had fully bleached (Fig. 3C). No significant difference in colony density was observed for the inocula corresponding to cultures sampled prior to CBQ and duroquinone addition, verifying that identical numbers of live cells were present in all cultures (Fig. 3C). It therefore appears that duroquinone possesses genuine bactericidal activity towards *Synechocystis* when present at a concentration as low as 10 μM, comparable to the effectiveness of antibiotics, while at the same concentration CBQ acts only as a mild bacteriostat.

2.3. Duroquinone impairs photosynthesis in arabidopsis

When added to solid Musharige & Skoog medium, duroquinone inhibited the growth of Arabidopsis plants (Fig. 4). Here again, duroquinone displayed pronounced cytotoxicity already at 10 μM (Fig. 4). However, unlike the situation observed with *Synechocystis*, none of the other tested benzoquinones had any visible impact on Arabidopsis growth (Supplemental Fig. 1).

Measurement of photosynthetic parameters showed that after 10 days of treatment, the maximum quantum efficiency of leaves from duroquinone-treated plants was significantly lower than that of the controls, resulting in lower photosynthetic efficiency (Table 1). Duroquinone-treated plants also exhibited a collapse in chlorophyll *a* fluorescence decline ratio (R_{fd}; Table 1), indicating that net CO_2 assimilation was severely hindered (Lichtenthaler and Miehé, 1997). Such decreases in maximum quantum efficiency and chlorophyll *a* fluorescence decline ratio are remindful of those observed in plastoquinone-9 biosynthetic mutants and methyl-plastoquinone-9-accumulating transgenics, the plastoquinone-9 pools of which had been severely depleted (Block et al., 2014; Stutts et al., 2023). A small decrease in chlorophyll *a* fluorescence decline ratio (R_{fd}) was also measured for the CBQ-treated plants as compared to the controls (Supplemental Table 1).

2.4. Duroquinone treatment results in decreased levels of chlorophyll and β-carotene, but has effect on plastoquinone-9 content

To further investigate the mechanism of duroquinone-induced photosynthetic inhibition in Arabidopsis, the leaves of ten-day-old plants grown in presence of duroquinone were subjected to metabolite profiling targeted to photosynthetic cofactors and pigments. The monitored metabolites included chlorophylls *a and b*, plastoquinone-9 (reduced and oxidized), plastochromanol-8, the cyclized product of plastoquinol-9 via the action of tocopherol cyclase (Kruk et al., 2014), α- and γ-tocopherols, which share homogentisate as a biosynthetic

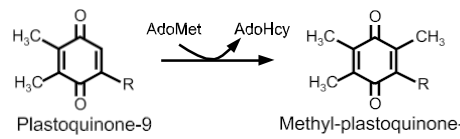

Fig. 1. Conversion of plastoquinone-9 into methyl-plastoquinone-9 by substrate promiscuous quinol *C*-methyltransferase COQ5. Note that methyl-plastoquinone-9 is highly cytotoxic to oxygenic phototrophs and is not known to occur in nature. It can, however, be transiently produced by metabolic engineering in cyanobacteria and plastids. AdoMet, S-adenosyl-L-Methionine; AdoHcy, S-adenosyl-L-Homocysteine; R, Solanesyl.

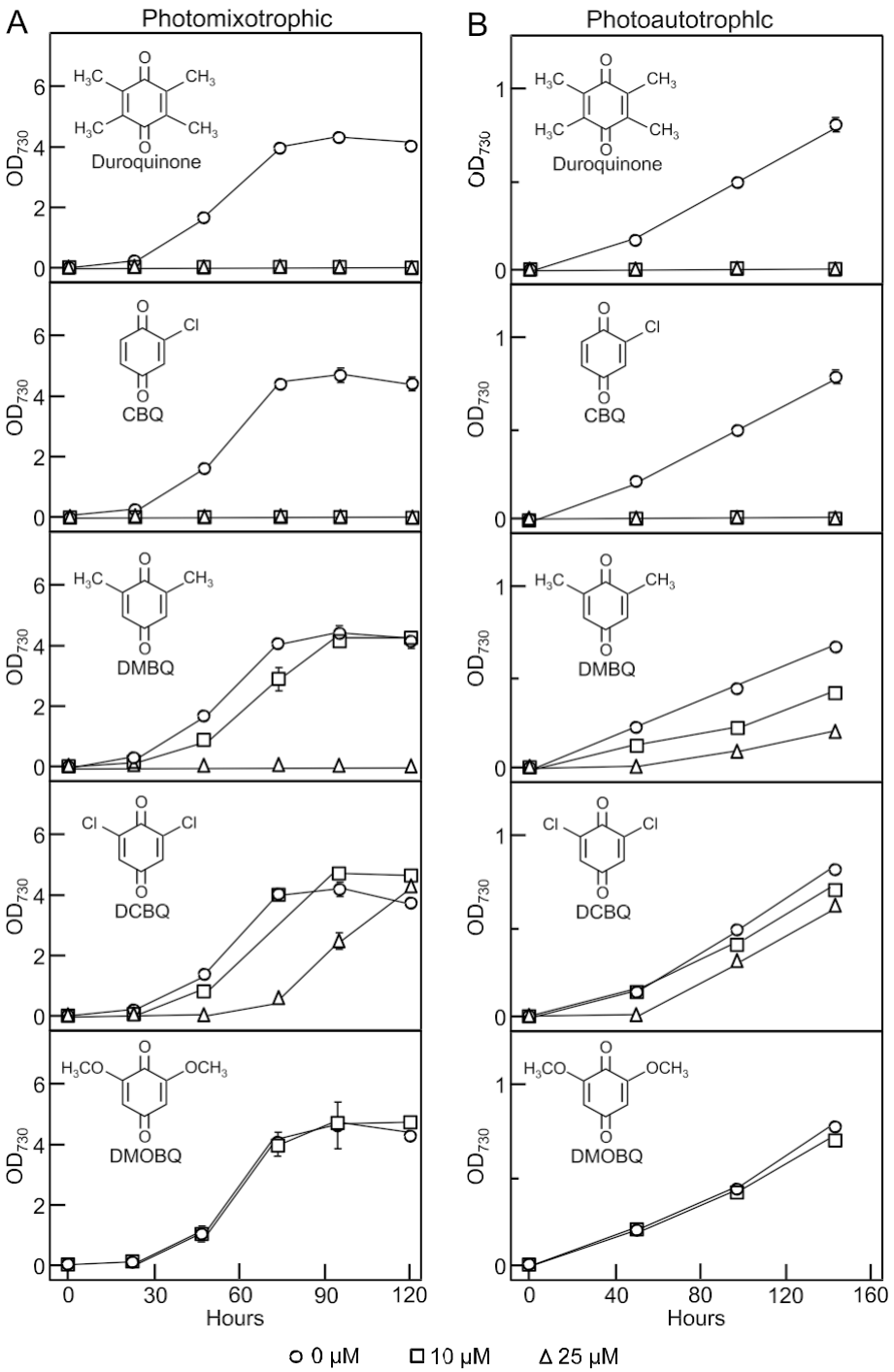

Fig. 2. Growth curves of *Synechocystis* sp. PCC 6803. A) *Synechocystis* cells were grown in liquid BG-11 medium containing glucose (photomixotrophic conditions) in presence (10 or 25 μM) or absence (0 μM) of the unprenylated benzoquinones 2,3,5,6-tetramethyl-1,4-benzoquinone (duroquinone), 2-chloro-1,4-benzoquinone (CBQ), 2,6-dimethyl-1,4-benzoquinone (DMBQ), 2,6-dichloro-1,4-benzoquinone (DCBQ), and 2,6-dimethoxy-1,4-benzoquinone (DMOBQ). B) Same as in A) except that *Synechocystis* cells were grown without glucose (photoautrophic conditions). Open circles (0 μM benzoquinones), open squares (10 μM benzoquinones), open triangles (25 μM benzoquinones). Note that the poor solubility of DMOBQ prevented its testing at 25 μM. Data represent the means of two biological replicates ± SD.

precursor with plastoquinone-9 (Fiedler et al., 1982), the carotenoids, phytoene and β-carotene, and phylloquinone, which serves as a light-dependent electron carrier from chlorophyll *a* to the iron-sulfur cluster Fx in photosystem I (Sigfridsson et al., 1995). Chlorophyll content was decreased by half in duroquinone-treated plants as compared to the controls (Fig. 5A). As expected, such a drop in chlorophyll content was paralleled by a pronounced boost in the level of α-tocopherol (Fig. 5B), the phytyl moiety of which is known to serve as a sink for the salvaging of phytol released during chlorophyll degradation (Vom Dorp et al., 2015). Plastochromanol-8 level increased by ~40 % in duroquinone-treated plants (Fig. 5B). This result could be explained by an increase in the reduction of plastoquinone-9 or an increase in tocopherol cyclase activity or both. Total plastoquinone-9 content in duroquinone-treated plants was not statistically different from that of the controls, indicating that duroquinone toxicity does not directly result from the inhibition of plastoquinone-9 biosynthesis (Fig. 5C).

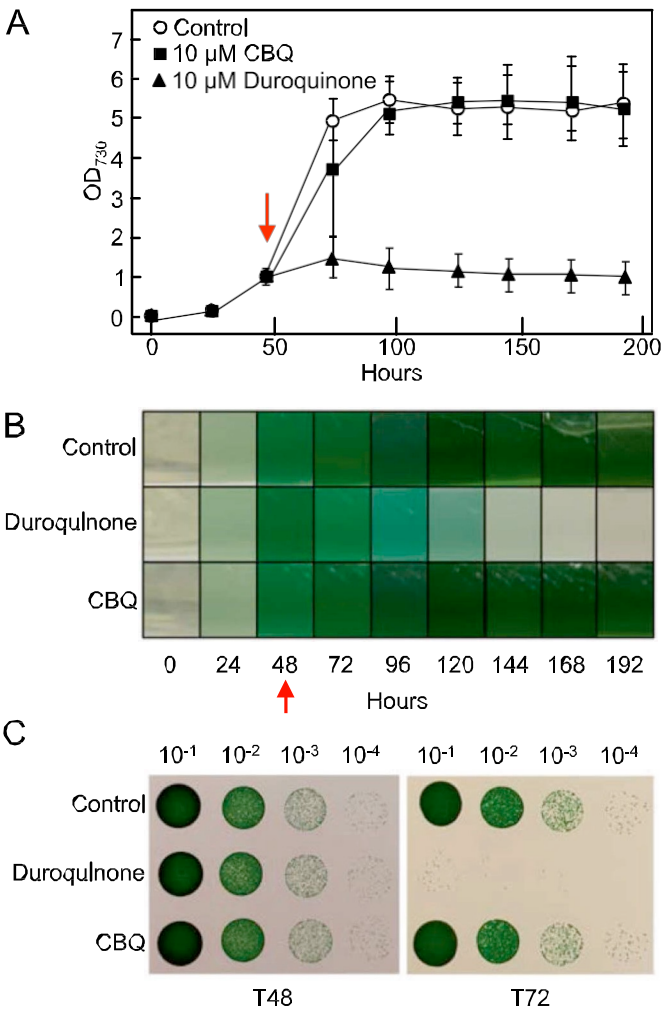

Fig. 3. Tests of the bactericidal activity vs. bacteriostatic activity of duroquinone and CBQ on *Synechocystis* sp. PCC 6803. A) Growth curves of *Synechocystis* cells in liquid BG-11 medium containing glucose, with or without (control) duroquinone or CBQ. The vertical red arrow indicates addition of duroquinone or CBQ at T48 h. Data represent the means of two biological replicates ± SD. B) Imaging of the cell cultures corresponding to the growth curves shown in A). C) Serial dilution growth assays of *Synechocystis* cells on solid BG-11 medium containing glucose. Cells were harvested immediately prior to (T48) and 24h after (T72) the addition of CBQ and duroquinone, washed, and then quantified by absorbance. Initial inocula contained identical numbers of cells. Plates were imaged after 9 days.

β-carotene content was decreased by ~50% in duroquinone-treated plants as compared to the control, suggesting a possible loss of photosystems (Fig. 5D). That chlorophyll content in duroquinone-treated plants decreased by a similar level (Fig. 5A) is congruent with this hypothesis. Similar symptoms are observed in response to DCMU-treatment, which is known to trigger photodestruction of β-carotene and chlorophyll-protein complexes (Ridley, 1977). Our data do not support the scenario of an inhibition of *plastid terminal oxidase*, the enzyme that couples plastoquinol-9 re-oxidation to carotenoid biosynthesis via the activity of phytoene desaturase (Carol et al., 1999). Indeed, in contrast to the Arabidopsis *plastid terminal oxidase* mutant, which accumulates phytoene (Wetzel et al., 1994), no statistically significant difference in phytoene content was observed between duroquinone-treated plants and the controls (Fig. 5D). Similarly, duroquinone-treated plants did not display the variegation phenotype that typifies *plastid terminal oxidase* knockout mutants (Wetzel et al., 1994). No methyl-plastoquinone-9 was detected confirming that duroquinone is not prenylated *in vivo*. No statistically significant difference

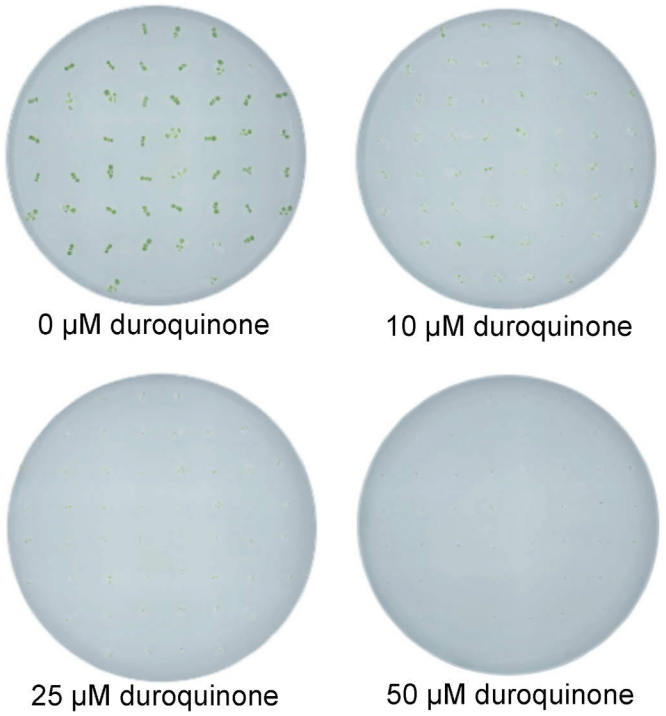

Fig. 4. Growth inhibition of Arabidopsis by duroquinone. Ten-day-old Arabidopsis plants (Col-0) were grown on MS medium containing 1% sucrose (w/v) and 0, 10, 25, or 50 μM duroquinone.

Table 1
Fluorescence parameters of Arabidopsis rosette leaves.

	0 μM (Control)	10 μM duroquinone
Fv/Fm	0.786± 0.002	0.626± 0.006*
R_{fd}	0.502± 0.017	−0.014 ± 0.033*
Damage to PSII (%)	–	20.356± 0.763*

Values are from 5 experimental replicates each comprising 4 biological replicates ± SE. Asterisks indicate significant differences from the control plants as determined by Fisher's test ($p < 0.05$) from an analysis of variance.

in the contents of phylloquinone and γ-tocopherol was observed in duroquinone-treated plants as compared to the controls (Fig. 5B).

2.5. Duroquinone concentrations that are lethal for cyanobacteria and plants do not impact the growth of Escherichia coli and yeast

To examine to what extent the cytotoxicity of duroquinone was specific to oxygenic phototrophs, duroquinone was added to cultures of *E. coli* and yeast (*Saccharomyces cerevisiae*) at the same final concentrations (10 and 25 μM) for which lethal effects were observed in *Synechocystis* and Arabidopsis (Fig. 6). For both *E. coli* and yeast, no significant difference in growth was observed between the cultures containing duroquinone and their corresponding controls (Fig. 6). Although duroquinone is known to serve as a generalist electron carrier for various oxidoreductases, including those associated with the mitochondrial respiratory chain and the plasma membrane (Ruzicka and Crane, 1971; Zhu and Beattie, 1988; Valenti et al., 1990), our data indicate that duroquinone is significantly more toxic to oxygenic phototrophs than to non-photosynthetic bacteria and yeast. Similarly, duroquinone has been shown to trigger the production of reactive oxygen species in mammalian cells (Canchola et al., 2022; Wu and O'Shea, 2020), however, one should emphasize that this effect has been observed for concentrations of duroquinone more than three orders of magnitude higher than those used in the present study.

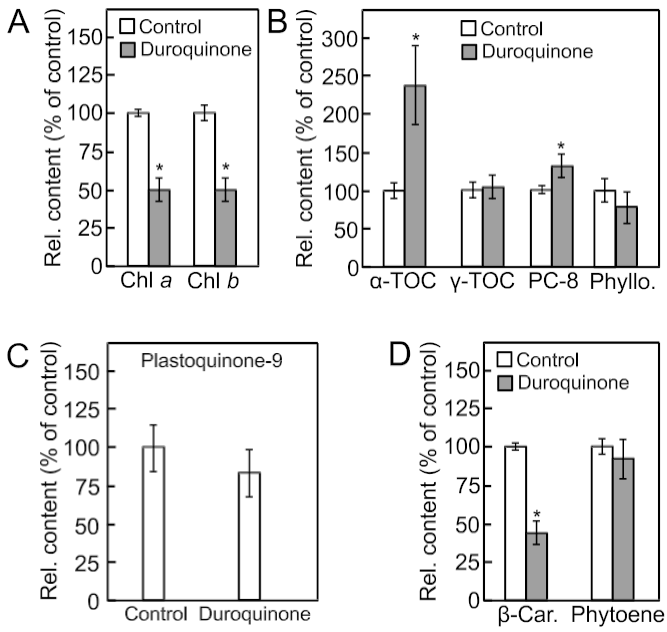

Fig. 5. Metabolite content in the rosette leaves of *in vitro* grown Arabidopsis plants. A) Chlorophyll *a* (chl *a*) and chlorophyll *b* (chl *b*). B) α-tocopherol (α-Toc), γ-tocopherol (γ-Toc), plastochromanol-8 (PC-8), phylloquinone (Phyllo.). C) Plastoquinone-9. Bars represent total plastoquinone-9 *i.e.* quinone and quinol forms. D) β-carotene (β-Car.) and phytoene. Data are means of four biological replicates ± SE. Asterisks indicate significant differences from control plants (no duroquinone treatment) as determined by Fisher's test ($p < 0.1$) from an analysis of variance.

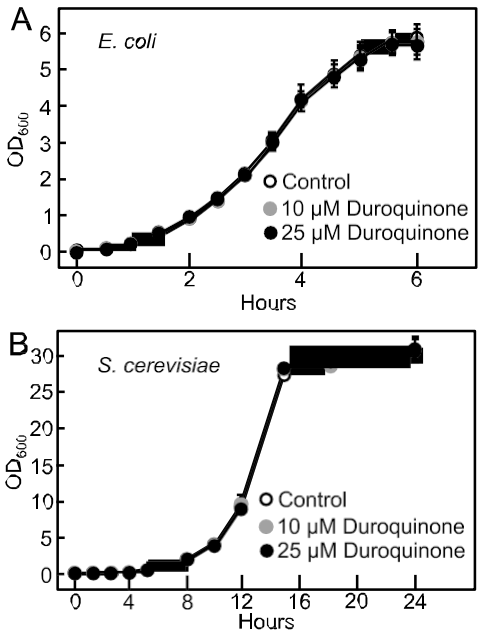

Fig. 6. Growth curves of *Escherichia coli* and *Saccharomyces cerevisiae*. Cells were grown in LB medium at 37 °C (*E. coli*) or YPD medium (*S. cerevisiae*) at 30 °C with (10 or 25 μM) or without (duroquinone). Data represent the means of two biological replicates ± SD. Open circles (0 μM duroquinone), grey circles (10 μM duroquinone), black circles (25 μM duroquinone).

3. Conclusions

Out of the five unprenylated benzoquinones tested in this study, duroquinone, CBQ, DMBQ, DCBQ, and DMOBQ, duroquinone most consistently and effectively mimics the antimetabolite activity of methyl-plastoquinone-9 towards plastoquinone-9 in both *Synechocystis* and Arabidopsis. This finding implies that prenylation of the benzoquinone ring in *ortho* of the methyl is not required for cytotoxicity; such a feature not only considerably facilitates the synthesis of the inhibitor at scale, but also likely its uptake by plant cells and cyanobacteria. As plastoquinone-9 is required for numerous key cellular processes in oxygenic phototrophs, including operation of the photosynthetic electron transfer chain, redox sensing and signaling, scavenging of reactive oxygen species, and carotenoid biosynthesis (Havaux, 2020), it is likely that duroquinone owes its cytotoxicity to pleiotropic effects.

This proof-of-concept study shows that usage of duroquinone for managing herbicide-resistant weeds as well as for mitigating cyanobacterial blooms merits further investigations in the field. In particular, since duroquinone is stable for several days in aqueous solutions, it offers prospects for preventive control of cyanobacterial blooms when standard management practices, such as reduction in nutrient load, are not feasible.

4. Experimental

4.1. Chemicals and reagents

Ubiquinone-9, ubiquinone-10, α-tocopherol, γ-tocopherol, duroquinone, 2,6-dimethlybenzoquinone, 2,6-dimethoxy-1,4-benzoquinone, 2,6-dichloro-1,4-benzoquinone and 2-chloro-1,4-benzoquinone were from Sigma-Aldrich. Plastoquinone-9 and plastochromanol-8 were HPLC-purified from Arabidopsis leaf extracts (Block et al., 2013). Plastoquinol and ubiquinol standards were prepared by reduction of their corresponding quinone versions with sodium borohydride. Phytoene was obtained from the white sectors of the leaves of the Arabidopsis *immutans* (Wetzel et al., 1994). β-Carotene was from Alfa Aesar. Phylloquinone and Murashige and Skoog medium were from MP Biomedicals, LLC. Unless mentioned otherwise, other reagents were from Fisher Scientific.

4.2. Biological material and growth conditions

Synechocystis sp PCC 6803 was cultured in BG-11 medium with (photomixotrophic conditions) or without (photoautotrophic conditions) 5 mM glucose in continuous light (50 μmol photons $m^{-2}s^{-1}$) at 30 °C. For growth assays in liquid medium, 3 day-old photomixotrophic or 11 day-old photoautotrophic starter cultures in exponential phase were used to inoculate corresponding 25 ml cultures ($OD_{730\ nm} = 0.05$) with shaking (125 rpm). For recovery assays on plates, liquid culture aliquots were harvested (5 min; 2200×*g*), cell pellets were washed 3 times with BG-11 medium, and resuspended cells (~1 ml) were spotted via serial dilutions (OD_{730} = of 0.1, 0.01, 0.001, or 0.0001) on BG-11 solid medium and grown photomixotrophically for 9 days at 24 °C. Pilot experiments showed there was no difference in benzoquinone toxicity at 24 °C and at 30 °C. *Arabidopsis thaliana* (Columbia-0) was germinated on Murashige and Skoog agar plates supplemented with 1% (w/v) sucrose and grown for 10 days at a light intensity of 110 μmol photons $m^{-2}s^{-1}$ in 12-h days at 22 °C. For *E. coli* and *S. cerevisiae* growth assays, overnight starter cultures were used to inoculate 25 ml cultures ($OD_{600\ nm} = 0.05$) of LB and YPD media, respectively. Cell cultures were carried out at 37 °C (*E. coli*) and 30 °C (yeast) with shaking (245 rpm). Quinone analogues (oxidized forms) were prepared in 95% (v/v) ethanol resulting in a final concentration of ethanol in the cell or plant cultures of 0.0095% (v/v). Ethanol was added at the same final concentration to the control treatments.

4.3. Metabolite analyses

Analyses of plastoquinone, phylloquinone, tocopherols, chlorophylls, and carotenoids were performed on flash-frozen leaf tissues

(14–37.9 mg) of 10-days-old Arabidopsis seedlings. Samples were homogenized in 0.5 ml of 95% (v/v) ethanol using a 5-ml Pyrex tissue grinder. The grinder was washed with 0.2 ml of 95% (v/v) ethanol, and the wash was combined with the original extract. The sample was then centrifuged (5 min; 18,000×*g*) and immediately analyzed by reverse-phase HPLC on a 5 μM Supelco Discovery C-18 column (250 × 4.6 mm, Sigma-Aldrich) thermostatted at 30 °C and developed in isocratic mode at a flow rate of 1.5 ml min^{-1} with 100% methanol. Compounds were monitored either via diode array spectrophotometry (phylloquinone, 246 nm; plastoquinone-9, 255 nm; phytoene, 286 nm; chlorophyll *a*, 432 nm; carotenoids, 440 nm; and chlorophyll *b*, 470 nm) or via fluorescence (plastoquinol-9, plastochromanol-8, and tocopherols; 290 nm excitation and 330 nm emission). Retention times were 5.1 min (chlorophyll *b*), 5.4 min (γ-tocopherol), 6 min (α-tocopherol), 7.7 min (chlorophyll *a*), 9.4 min (phylloquinone), 13.1 min (plastoquinol-9), 21.9 min (phytoene), 22.6 min (β-carotene), 26 min (plastochromanol-8), and 37.1 min (plastoquinone-9).

4.4. Measurements of photosynthetic parameters

Induction, detection, and analyses of chlorophyll fluorescence were performed on dark-adapted (20 min) 10-day-old Arabidopsis seedlings using a FluorCam 800 MF imaging system and its associated software (Photon Systems Instruments). Fluorescence parameters were calculated as follows: Maximum quantum yield of PSII, $QY\_max = (F_M - F_0)/F_M$, where F_M is the measured maximum fluorescence in dark-adapted state, and F_0 is the measured minimum fluorescence in dark-adapted state; fluorescence decline ratio in steady-state, which linearly correlates with net CO_2 assimilation (Lichtenthaler and Miehé, 1997), $R_{fd} = (F_P - F_{t\_Lss})/F_{t\_Lss}$, where F_P is the peak fluorescence measured during the initial phase of the Kautsky effect and F_{t_Lss} is the measured steady-state fluorescence in the light; Damage to PSII = 1-(QY_max (inhibitor)/QY_max (Mock)).

Funding

This work was supported by National Science Foundation Grant MCB-2216747; and the Florida Nursery, Growers and Landscape Association Endowed Research Fund.

CRediT authorship contribution statement

Scott Latimer: Writing – original draft, Methodology, Investigation, Data curation, Conceptualization. **Lauren R. Stutts:** Investigation, Formal analysis, Data curation, Conceptualization. **Gilles J. Basset:** Writing – review & editing, Writing – original draft, Supervision, Resources, Project administration, Methodology, Investigation, Funding acquisition, Formal analysis, Data curation, Conceptualization.

Declaration of competing interest

The authors declare that they have no known competing financial interests or personal relationships that could have appeared to influence the work reported in this paper.

Data availability

Data will be made available on request.

Appendix A. Supplementary data

Supplementary data to this article can be found online at https://doi.org/10.1016/j.phytochem.2024.114225.

References

Block, A., Fristedt, R., Rogers, S., Kumar, J., Barnes, B., Barnes, J., Elowsky, C.G., Wamboldt, Y., Mackenzie, S.A., Redding, K., Merchant, S.S., Basset, G.J., 2013. Functional modeling identifies paralogous solanesyl-diphosphate synthases that assemble the side chain of plastoquinone-9 in plastids. J. Biol. Chem. 288, 27594–27606. https://doi:10.1074/jbc.M113.492769.

Block, A., Widhalm, J.R., Fatihi, A., Cahoon, R.E., Wamboldt, Y., Elowsky, C., Mackenzie, S.A., Cahoon, E.B., Chapple, C., Dudareva, N., Basset, G.J., 2014. The origin and biosynthesis of the benzenoid moiety of ubiquinone (Coenzyme Q) in Arabidopsis. Plant Cell 26, 1938–1948. https://doi.org/10.1105/tpc.114.125807.

Boler, J., Pardini, R., Mustafa, H.T., Folkers, K., Dilley, R.A., Crane, F.L., 1972. Synthesis of plastoquinone analogs and inhibition of photosynthetic and mammalian enzyme systems. Proc. Natl. Acad. Sci. USA 69, 3713–3717. https://doi:10.1073/pnas.69.12.3713.

Canchola, A., Ahmed, C.M.S., Chen, K., Chen, J.Y., Lin, Y.H., 2022. Formation of redox-active duroquinone from vaping of vitamin E acetate contributes to oxidative lung injury. Chem. Res. Toxicol. 35, 254–264. https://doi:10.1021/acs.chemrestox.1c00309.

Carol, P., Stevenson, D., Bisanz, C., Breitenbach, J., Sandmann, G., Mache, R., Coupland, G., Kuntz, M., 1999. Mutations in the Arabidopsis gene IMMUTANS cause a variegated phenotype by inactivating a chloroplast terminal oxidase associated with phytoene desaturation. Plant Cell 11, 57–68. https://doi.org/10.1105/tpc.11.1.57.

Duke, S.O., Dayan, F.E., 2022. The search for new herbicide mechanisms of action: is there a 'holy grail'? Pest Manag. Sci. 78, 1303–1313. https://doi:10.1002/ps.6726.

Fiedler, E., Soll, J., Schultz, G., 1982. The formation of homogentisate in the biosynthesis of tocopherol and plastoquinone in spinach chloroplasts. Planta 155, 511–515. https://doi:10.1007/BF01607575.

Gerhards, R., Dentler, J., Gutjahr, C., Auburger, S., Bahrs, E., 2016. An approach to investigate the costs of herbicide-resistant Alopecurus myosuroides. Weed Res. 56, 407–414. https://doi.org/10.1111/wre.12228.

Havaux, M., 2020. Plastoquinone in and beyond photosynthesis. Trends Plant Sci. 25, 1252–1265. https://doi:10.1016/j.tplants.2020.06.011.

Huisman, J., Codd, G.A., Paerl, H.W., Ibelings, B.W., Verspagen, J.M.H., Visser, P.M., 2018. Cyanobacterial blooms. Nat. Rev. Microbiol. 16, 471–483. https://doi:10.1038/s41579-018-0040-1.

Kahlau, S., Schröder, F., Freigang, J., Laber, B., Lange, G., Passon, D., Kleeßen, S., Lohse, M., Schulz, A., von Koskull-Döring, P., Klie, S., Gille, S., 2020. Aclonifen targets solanesyl diphosphate synthase, representing a novel mode of action for herbicides. Pest Manag. Sci. 76, 3377–3388. https://doi:10.1002/ps.5781.

Kosten, S., Huszar, V.L.M., Bécares, E., Costa, L.S., van Donk, E., Hansson, L.-A., Jeppesen, E., Kruk, C., Lacerot, G., Mazzeo, N., De Meester, L., Moss, B., Lürling, M., Nõges, T., Romo, S., Scheffer, M., 2012. Warmer climates boost cyanobacterial dominance in shallow lakes. Global Change Biol. 18, 118–126. https://doi.org/10.1111/j.1365-2486.2011.02488.x.

Kruk, J., Szymańska, R., Cela, J., Munne-Bosch, S., 2014. Plastochromanol-8: fifty years of research. Phytochemistry 108, 9–16. https://doi.org/10.1016/j.phytochem.2014.09.011.

Lichtenthaler, H.K., Miehé, J.A., 1997. Fluorescence imaging as a diagnostic tool for plant stress. Trends Plant Sci. 2, 316–320. https://doi.org/10.1016/S1360-1385(97)89954-2.

Lürling, M., Meng, D., Faassen, E.J., 2014. Effects of hydrogen peroxide and ultrasound on biomass reduction and toxin release in the cyanobacterium, *Microcystis aeruginosa*. Toxins 6, 3260–3280. https://doi.org/10.3390/toxins6123260.

Merel, S., Walker, D., Chicana, R., Snyder, S., Baurès, E., Thomas, O., 2013. State of knowledge and concerns on cyanobacterial blooms and cyanotoxins. Environ. Int. 59, 303–327.

Metz, J.G., Pakrasi, H.B., Seibert, M., Arntzer, C.J., 1986. Evidence for a dual function of the herbicide-binding D1 protein in photosystem II. FEBS Lett. 205, 269–274. https://doi.org/10.1016/0014-5793(86)80911-5.

Nowicka, B., Kruk, J., 2016. Cyanobacteria use both p-hydroxybenzoate and homogentisate as a precursor of plastoquinone head group. Acta Physiol. Plant. 38, 49. https://doi.org/10.1007/s11738-015-2043-0.

Oettmeier, W., Soll, H.-J., Neumann, E., 1984. Herbicide and plastoquinone binding to photosystem II. Z. Naturforsch. C Biosci. 39, 393–396. https://doi.org/10.1515/znc-1984-0517.

Paerl, H.W., Paul, V.J., 2012. Climate change: links to global expansion of harmful cyanobacteria. Water Res. 46, 1349–1363. https://doi:10.1016/j.watres.2011.08.002.

Peterson, M.A., Collavo, A., Ovejero, R., Shivrain, V., Walsh, M.J., 2018. The challenge of herbicide resistance around the world: a current summary. Pest Manag. Sci. 74, 2246–2259. https://doi:10.1002/ps.4821.

Powles, S.B., Yu, Q., 2010. Evolution in action: plants resistant to herbicides. Annu. Rev. Plant Biol. 61, 317–347. https://doi:10.1146/annurev-arplant-042809-112119. Ridley, S.M., 1977. Interaction of chloroplasts with inhibitors: induction of chlorosis by diuron during prolonged illumination in vitro. Plant Physiol. 59, 724–732. https://doi.org/10.1104/pp.59.4.724.

Ruzicka, F.J., Crane, F.L., 1971. Quinone interaction with the respiratory chain-linked NADH dehydrogenase of beef heart mitochondria. II. Duroquinone reductase activity. Biochim. Biophys. Acta, Bioenerg. 226, 221–233. https://doi.org/10.1016/0005-2728(71)90089-2.

Sigfridsson, K., Hansson, O., Brzezinski, P., 1995. Electrogenic light reactions in photosystem I: resolution of electron-transfer rates between the iron-sulfur centers. Proc. Natl. Acad. Sci. USA 92, 3458–3462. https://doi:10.1073/pnas.92.8.3458.

Sosnoskie, L.M., Culpepper, A.S., 2014. Glyphosate-resistant palmer amaranth (Amaranthus palmeri) increases herbicide use, tillage, and hand-weeding in Georgia cotton. Weed Sci. 62, 393–402. https://doi:10.1614/WS-D-13-00077.1.

Stutts, L., Latimer, S., Batyrshina, Z., Dickinson, G., Alborn, H., Block, A.K., Basset, G.J., 2023. The evolution of strictly monofunctional naphthoquinol C-methyltransferases is vital in cyanobacteria and plastids. Plant Cell 35, 3686–3696. https://doi:10.1093/plcell/koad202.

Tischer, W., Strotmann, H., 1977. Relationship between inhibitor binding by chloroplasts and inhibition of photosynthetic electron transport. Biochim. Biophys. Acta 460, 113–125. https://doi.org/10.1016/0005-2728(77)90157-8.

Valenti, V., Guerrini, F., Pupillo, P., 1990. NAD (P)H-duroquinone reductase in the plant plasma membrane. J. Exp. Bot. 41, 183–192. https://doi.org/10.1093/jxb/41.2.183.

Vom Dorp, K., Hölzl, G., Plohmann, C., Eisenhut, M., Abraham, M., Weber, A.P., Hanson, A.D., Dörmann, P., 2015. Remobilization of phytol from chlorophyll degradation is essential for tocopherol synthesis and growth of Arabidopsis. Plant Cell 27, 2846–2859. https://doi:10.1105/tpc.15.00395.

Wetzel, C.M., Jiang, C.Z., Meehan, L.J., Voytas, D.F., Rodermel, S.R., 1994. Nuclear-organelle interactions: the immutans variegation mutant of Arabidopsis is plastid autonomous and impaired in carotenoid biosynthesis. Plant J. 6, 161–175. https://doi:10.1046/j.1365-313x.1994.6020161.x.

Widhalm, J.R., van Oostende, C., Furt, F., Basset, G.J., 2009. A dedicated thioesterase of the Hotdog-fold family is required for the biosynthesis of the naphthoquinone ring of vitamin K1. Proc. Natl. Acad. Sci. U.S.A. 106, 5599–5603. https://doi:10.1073/pnas.0900738106.

Wu, D., O'Shea, D.F., 2020. Potential for release of pulmonary toxic ketene from vaping pyrolysis of vitamin E acetate. Proc. Natl. Acad. Sci. U.S.A. 117, 6349–6355. https://doi:10.1073/pnas.1920925117.

Zhu, Q.S., Beattie, D.S., 1988. The interaction of quinone analogues with wild-type and ubiquinone-deficient yeast mitochondria. Biochim. Biophys. Acta. 934, 303–313. https://doi.org/10.1016/0005-2728(88)90090-4.